PCCP

COMMUNICATION

Cite this: *Phys. Chem. Chem. Phys.*, 2018, **20**, 8456

Received 7th December 2017,
Accepted 12th March 2018

DOI: 10.1039/c7cp08209f

rsc.li/pccp

Modelling molecular adsorption on charged or polarized surfaces: a critical flaw in common approaches†

Kristof M. Bal * and Erik C. Neyts

A number of recent computational material design studies based on density functional theory (DFT) calculations have put forward a new class of materials with electrically switchable chemical characteristics that can be exploited in the development of tunable gas storage and electrocatalytic applications. We find systematic flaws in almost every computational study of gas adsorption on polarized or charged surfaces, stemming from an improper and unreproducible treatment of periodicity, leading to very large errors of up to 3 eV in some cases. Two simple corrective procedures that lead to consistent results are proposed, constituting a crucial course correction to the research in the field.

The chemical properties of electrocatalytic materials can be modified through charging or the application of electric fields. One such application is reversible gas adsorption: through addition or removal of electrons, the (relative) affinity of a nanomaterial for gas molecules can be changed, implying that charging can effectively be used as a switch in gas capture, storage, and separation technologies.[1] Furthermore, by tuning the charge state of a catalyst, its reactivity and selectivity can be tuned, which is suggested to be an important factor underpinning plasma-assisted catalysis.[2] Most of the work in this field has been based on theoretical investigations, where density functional theory (DFT) calculations consistently predict that extensive negative charging (*i.e.*, addition of electrons) greatly increases the selective adsorption of gasses such as CO_2 or H_2 on nanomaterials such as hexagonal boron nitride (h-BN),[3] graphitic carbon nitrides (such as g-C_3N_4 and g-C_4N_3),[4–7] doped graphene,[8] borophene,[9] and nanocomposites of these materials.[10] Similar switchable properties have also been demonstrated for electric fields by computational investigations of reversible gas adsorption[11–14] and processes relevant to catalysis.[15–17] Hence, computational design of materials with electrically switchable interfacial properties will play a major role in the development of new "green" technologies, where reversible gas capture and activation methods are required for carbon capture and sequestration, and the transport and storage of hydrogen gas.[18]

In order to make accurate predictions of charging-related material properties, the employed computational approaches must be adequate. Typically, models of adsorption and reactions on solid surfaces use small semi-infinite slabs, with periodic boundary conditions approximating the macroscopic surface. However, properties of systems with excess charges or large polarization are difficult to properly converge.[19] Furthermore, traditional computational approaches to charged periodic simulation cells have been found to be inadequate for inhomogeneous systems.[20] Indeed, these issues are well-known for charged defects in solids. A proper model of the bulk solid requires the application of periodic boundaries, but also introduces artificial long-ranged Coulomb interactions between the periodic images of the localized charges. Moreover, the inclusion of an implicit neutralizing background charge introduces unphysical contributions to the total energy, rendering a straightforward calculation of the defect formation energy impossible. For this situation, a number of techniques has been devised that allow to eliminate any spurious electrostatic interaction, *i.e.*, to treat the defect as isolated, embedded in a semi-infinite neutral matrix.[21–23]

Adsorption on charged surfaces poses a very different challenge. Indeed, because all periodic cells of interest—containing the pristine surface slab and adsorption complex, respectively—carry the same net charge, the effect of an implicit background charge is eliminated. Furthermore, the surface is assumed to be homogeneously charged, meaning that long-range interactions along periodic boundaries are a physically justifiable aspect of the model. However, full periodic boundary conditions (as usually applied) introduce an unphysical interaction of the material with itself, normal to its surface. In other words, the calculation cell dimensions along the surface directions have a physical meaning as they are a function of the material lattice parameters, but the edge length along the surface normal represents an arbitrary degree of freedom. To avoid spurious interactions from surface dipoles or charges, correction schemes exist, but the contemporary literature on electrochemically switchable adsorbents and catalysts does not adopt any specific corrective measures. Rather, sizable vacuum regions—as is also common practice in the study of

Department of Chemistry, University of Antwerp, Universiteitsplein 1, 2610 Antwerp, Belgium. E-mail: kristof.bal@uantwerpen.be

† Electronic supplementary information (ESI) available. See DOI: 10.1039/c7cp08209f

nonpolar or neutral surfaces—have been claimed to be sufficient without explicit confirmation of the adequacy of this approach.[3–16] In other words, the comparatively new field of charge- and field-tunable surface chemistry has not yet adopted a rigorous, consistent and properly validated standard computational procedure.

In this contribution we therefore revisit three prominent applications of switchable CO_2 capture from the literature as representative case studies for the modelling challenges posed by charged surfaces. Specifically, we consider charge-enhanced adsorption on g-C_4N_3 (a half metal)[5] and h-BN (a wide-gap semiconductor)[3] as well as electric field-tuned adsorption, again on h-BN.[13]

For all calculations, the Quickstep module in the CP2K 4.1 package[24,25] was adopted within the Gaussian and plane wave (GPW) framework,[26] employing Goedecker–Teter–Hutter (GTH) pseudopotentials[27,28] for the core–valence interactions and a polarized double-ζ (m-DZVP) basis set[29] to expand the Kohn–Sham valence orbitals. An auxiliary plane wave basis set was used to expand the electron density, defined by a cutoff of 1000 Ry. The PBE exchange and correlation functional[30] was used, supplemented by Grimme's D3 dispersion correction[31] in its Becke–Johnson damping form.[32] Atomic partial charges were calculated by the self-consistent Hirshfeld-I scheme.[33] All energies are reported without thermal or zero-point energy corrections, and adsorption energies on the nanosheet are defined as $E_{ads} = E_{mol+sheet} - E_{mol} - E_{sheet}$ so that a negative E_{ads} corresponds to a stable adsorption configuration.

Two different periodicities were considered: fully periodic calculations employed the default CP2K Poisson solver for electrostatics, whereas the Martyna–Tuckerman (MT) solver[34] allowed to impose two periodic (along the surface, *XY* plane) and one nonperiodic direction (along the surface normal, *Z* direction). Unless noted otherwise, geometries were optimized in cells with a nonperiodic *Z* length of 25 Å and used in single point energy calculations in all other cells. The MT solver is a reciprocal space-based method to calculate electrostatic energies that also allows treating both isolated and periodically replicated systems within the same formalism. As a consequence, systems with mixed boundary conditions can be studied. The MT solver has one specific limitation that must be kept in mind: the cell length along any nonperiodic axis must be at least two times the size of the charge distribution (incl. ions and electrons) of the system along this direction. For all of our systems, this means that the MT solver cannot be applied for very small vacuum spaces such as 10 Å.

Because these systems have already been characterized by DFT calculations, adsorption structures and relevant charge or field conditions can initially be directly taken from the literature. For charged g-C_4N_3, a charge state equivalent to $1e^-$ in a 2×2 supercell, as used in the literature, is considered; to compensate for the lack of *k* point sampling beyond the Γ point in our calculations we use a larger 4×4 supercell (Fig. 1a), with a $4e^-$ charge. An h-BN sheet was modelled as a 6×6 supercell (Fig. 1b), either carrying a $2e^-$ charge or subjected to an electric field of 0.04 a.u. (about 2 V Å^{-1}). In all cases, the considered charge levels or field strength have been reported to lead to a shift of the CO_2 adsorption mode from physisorption to chemisorption. The relevant adsorption structures for these systems are depicted in Fig. 1c–e.

The only "free" computational parameter with no true physical analogue is the vacuum space between the repeated periodic images

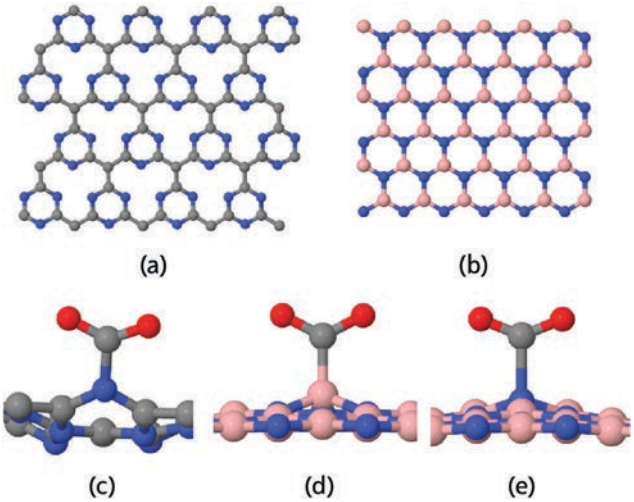

Fig. 1 Investigated CO_2 adsorption configurations. The two considered adsorbents are (a) a 4×4 g-C_4N_3 sheet and (b) 6×6 h-BN. The molecule is adsorbed on (c) $4e^-$ charged g-C_4N_3, (d) $2e^-$ charged h-BN, and (e) h-BN subjected to an electric field of 0.04 a.u., pointing downward. All configurations have been previously described in the literature. Atom color codes: gray, carbon; blue, nitrogen; pink, boron; red, oxygen.

of the adsorbent material, *i.e.*, the *Z* length of the simulation cell. Therefore, we first perform adsorption energy calculations using different sizes of the vacuum region, for both the pristine sheet and the adsorption complex, to assess its impact. In Fig. 2a, these energies are plotted for CO_2 adsorption on charged g-C_4N_3, demonstrating the huge impact of the vacuum region. Depending on the imposed intersheet spacing, the interaction of CO_2 with the sheet is either predicted to be very favorable (with a strongly negative adsorption energy), or not binding at all, which means that not only quantitative predictions, but even qualitative trends are sensitive to the vacuum size. Furthermore, no clear convergence is observed, even when using a very large cell length of 50 Å, which is significantly larger than the commonly reported vacuum sizes of 15–25 Å.

One way to avoid the problem of periodic images interacting with each other is to use specialized Poisson solvers for electrostatics, that allow to mix periodic and nonperiodic boundaries. We repeat the adsorption energy calculations in different cell sizes, but now apply the MT solver[34] to impose nonperiodic boundaries along the *Z* direction. This setup gives rise to adsorption energies independent of the cell dimensions, as expected (Fig. 2a). If the adsorption energy obtained in a partially nonperiodic cell is assumed to reflect the properly converged solution, it can be inferred that calculations in fully periodic cells consistently underestimate this property, even when large vacuum sizes are used. This can be understood as follows: significant charge transfer toward the adsorbed molecule takes place upon adsorption, and the region carrying a net charge becomes "thicker" compared to the pristine "clean" nanosheet. The repulsive interaction between periodic images of clean sheets can be expected to be proportional to L^{-1}, with *L* the vacuum spacing along the *Z* direction. The effective separation between sheets carrying adsorbed molecules, then, is reduced. For large *L*, the as such introduced error will be simply proportional to L^{-1}, and extrapolation $L \to \infty$ should give adsorption energies free of any error. Indeed, as depicted in

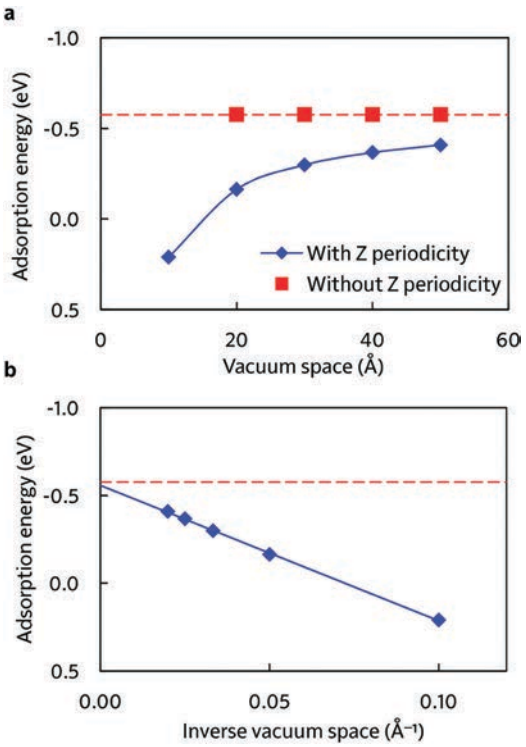

Fig. 2 Convergence dependence of CO_2 adsorption energies on charged g-C_4N_3 on the vacuum size. (a) Dependence of the adsorption energy on the vacuum space for both fully as partially periodic cells. (b) Extrapolation to infinite vacuum. Details can be found in the text.

Fig. 2b, extrapolated adsorption energies from fully periodic cells are identical to the solution obtained in a cell with partial periodicity, also confirming the appropriateness of the latter.

The same detailed treatment for the other systems is given in the ESI,† and some key results are summarized in Fig. 3. Similar to g-C_4N_3, the effect of charge-enhanced adsorption on h-BN is significantly underestimated in fully periodic cells: the commonly applied vacuum space of 20 Å gives rise to a significant error of 0.44 eV, and even an impractically large cell edge length of 50 Å still is still off by 0.18 eV. Furthermore, the error increases with the magnitude of the surface charge, as depicted in Fig. 4. Evidently, such a large charge-dependent

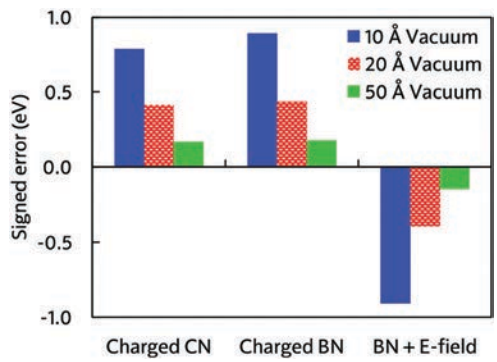

Fig. 3 Absolute signed errors for adsorption energies in all systems for various vacuum sizes. As a reference, energies obtained from partially periodic calculations are used.

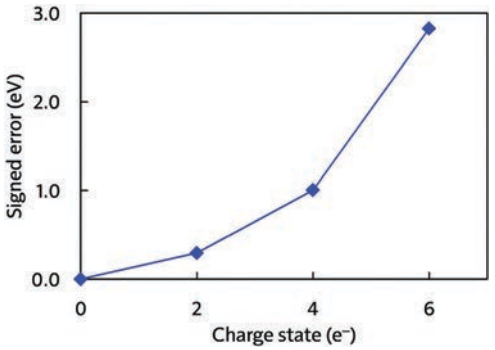

Fig. 4 Absolute signed errors for adsorption energies on h-BN in different charge states in a fully periodic box with a vacuum of 30 Å. As a reference, energies obtained from partially periodic calculations are used.

error renders computational studies with improper periodicity that compare the properties of different charge states[1,4–7,10] useless.

A somewhat different picture arises for electric field-modulated adsorption. Here, fully periodic cells tend to overstabilize adsorbed CO_2. This can be explained by the difference in interaction across periodic images, which is not a charge-charge repulsion, but an attractive dipole–dipole attraction. Electric field-enhanced adsorption of CO_2 relies on a large polarization effect from the electric field to push electrons from the nanosheet into the molecule, which causes the adsorption complex to have a larger induced dipole, and hence stronger interactions across periodic boundaries than the pristine nanosheet, where electrons have nowhere else to go. Nevertheless, energies from the fully periodic cells can also be extrapolated to the partially periodic result for this system, as shown in Fig. S4 (ESI†).

While energetics are strongly affected by the treatment of periodicity, electronic structures of the considered systems are fairly insensitive to it. For example, the charge transfer to CO_2 (as an indication of the relevant electronic structure) on charged h-BN is $1.187e^-$ in a converged calculation, and $1.175e^-$ in fully periodic system with a modest vacuum size of 20 Å. Similar observations for this transition can be made for h-BN subjected to an electric field ($0.523e^-$ to $0.554e^-$) and charged g-C_4N_3 ($0.416e^-$ to $0.383e^-$). These highly similar electron densities also imply a similar ground state structure, which indeed appears to be the case, at least for charge-enhanced adsorption. Reoptimization of the adsorption complex on charged g-C_4N_3 in a periodic cell with 25 Å vacuum yields a N–CO_2 bond of 1.53 Å, as compared to the 1.54 Å in the cell with partial periodicity, while the same strategy changes the B–CO_2 bond on charged h-BN from 1.67 to 1.66 Å. Structures generated by pure external field-driven adsorption are much more sensitive to the imposed periodicity. As demonstrated by the calculated adsorption energies on h-BN, interaction between periodic repeated images amplifies the effective external field, which should strengthen molecular binding. Indeed, the N–CO_2 bond length changes from 1.71 Å to 1.82 Å upon reducing periodicity. Periodicity errors in charge-enhanced adsorption therefore only appear to consist of an energetic term, whereas electric fields also produce different forces.

Unfortunately, we have been unable to cross-check our results with some of the relevant previous studies[5,13] because these are inherently unreproducible. Rather than reporting exact box dimensions, employed vacuum spacings are consistently reported as being

"larger than" a certain value, which is a very troubling carelessness that appears to permeate the literature.[4,5,8–10,13] Because results can be "tuned" by changing the vacuum spacing, such vague language is not acceptable since it makes comparison across materials, molecules, and DFT codes impossible. We could find well-defined computational results for charged h-BN, for which a vacuum distance of 15 Å was used.[3] For this separation, we find a CO_2 adsorption energy of −2.45 eV, in good agreement with the value of −2.32 eV in ref. 3. Compared to fully converged cell sizes that produce an adsorption energy of −3.04 eV, these results are in error by ∼0.6 eV, or 25%.

We have shown that conventional computational approaches to charge- and electric field-controlled gas capture, storage and conversion processes can give rise to significant artifacts due to incomplete convergence of interlayer interactions across periodic boundaries. These errors appear to affect the bulk of the literature on the subject.[3–16] In future work, fully converged adsorption energies can be obtained through one of two possible strategies: extrapolation of fully periodic calculations to infinite vacuum, or adoption of specialized Poisson solvers that also allow a nonperiodic direction along the surface normal. The former approach can be easily realized in any of the standard periodic DFT codes, whereas the latter will also be able to self-consistently yield converged minimum energy configurations and is hence preferred. In fact, many commonly available codes allow reduced 2D periodicities in calculations, and strategies to obtain accurate energetics are already available to most computational scientists. We stress that in general, calculations of fully periodic systems with large vacuum can correctly capture charge-modulated adsorption phenomena, but quantitative predictions for material design require properly converged adsorption energies. We hope that these recommendations will have a positive impact on the practical realization of flexible catalytic processes and high-performance gas capture technologies.

Conflicts of interest

There are no conflicts to declare.

Acknowledgements

K. M. B. is funded as PhD fellow (aspirant) of the FWO-Flanders (Research Foundation – Flanders), Grant 11V8915N. The computational resources and services used in this work were provided by the VSC (Flemish Supercomputer Center), funded by the FWO and the Flemish Government – department EWI.

References

1 X. Tan, H. A. Tahini and S. C. Smith, *Energy Storage Materials*, 2016, **8**, 169–183.
2 K. M. Bal, S. Huygh, A. Bogaerts and E. C. Neyts, *Plasma Sources Sci. Technol.*, 2018, **27**, 024001.
3 Q. Sun, Z. Li, D. J. Searles, Y. Chen, G. Lu and A. Du, *J. Am. Chem. Soc.*, 2013, **135**, 8246–8253.
4 X. Tan, L. Kou, H. A. Tahini and S. C. Smith, *ChemSusChem*, 2015, **8**, 3626–3631.
5 X. Tan, L. Kou, H. A. Tahini and S. C. Smith, *Sci. Rep.*, 2015, **5**, 17636.
6 X. Li, T. Guo, L. Zhu, C. Ling, Q. Xue and W. Xing, *Chem. Eng. J.*, 2018, **338**, 92–98.
7 G.-Q. Qin, A.-J. Du and Q. Sun, *Energy Technol.*, 2018, **6**, 205–212.
8 X. Tan, H. A. Tahini and S. C. Smith, *ACS Appl. Mater. Interfaces*, 2016, **8**, 32815–32822.
9 X. Tan, H. A. Tahini and S. C. Smith, *ACS Appl. Mater. Interfaces*, 2017, **9**, 19825–19830.
10 X. Tan, L. Kou and S. C. Smith, *ChemSusChem*, 2015, **8**, 2987–2993.
11 J. Zhou, Q. Wang, Q. Sun, P. Jena and X. S. Chen, *Proc. Natl. Acad. Sci. U. S. A.*, 2010, **107**, 2801–2806.
12 S. Lee, M. Lee and Y.-C. Chung, *Phys. Chem. Chem. Phys.*, 2013, **15**, 3243–3248.
13 H. Guo, W. Zhang, N. Lu, Z. Zhuo, X. C. Zeng, X. Wu and J. Yang, *J. Phys. Chem. C*, 2015, **119**, 6912–6917.
14 Q. Sun, G. Qin, Y. Ma, W. Wang, P. Li, A. Du and Z. Li, *Nanoscale*, 2017, **9**, 19–24.
15 A. A. Koverga, S. Frank and M. T. M. Koper, *Electrochim. Acta*, 2013, **101**, 244–253.
16 F. Che, J. T. Gray, S. Ha and J.-S. McEwen, *ACS Catal.*, 2017, **7**, 551–562.
17 A. Kakekhani and S. Ismail-Beigi, *Phys. Chem. Chem. Phys.*, 2016, **18**, 19676–19695.
18 S. Chu and A. Majumdar, *Nature*, 2012, **488**, 294–303.
19 G. Makov and M. C. Payne, *Phys. Rev. B: Condens. Matter Mater. Phys.*, 1995, **51**, 4014–4022.
20 J. S. Hub, B. L. de Groot, H. Grubmüller and G. Groenhof, *J. Chem. Theory Comput.*, 2014, **10**, 381–390.
21 H.-P. Komsa and A. Pasquarello, *Phys. Rev. Lett.*, 2013, **110**, 095505.
22 H.-P. Komsa, N. Berseneva, A. V. Krasheninnikov and R. M. Nieminen, *Phys. Rev. X*, 2014, **4**, 031044.
23 D. Vinichenko, M. G. Sensoy, C. M. Friend and E. Kaxiras, *Phys. Rev. B*, 2017, **95**, 235310.
24 J. VandeVondele, M. Krack, F. Mohamed, M. Parrinello, T. Chassaing and J. Hutter, *Comput. Phys. Commun.*, 2005, **167**, 103–128.
25 J. Hutter, M. Iannuzzi, F. Schiffmann and J. VandeVondele, *WIREs Comput. Mol. Sci.*, 2014, **4**, 15–25.
26 G. Lippert, J. Hutter and M. Parrinello, *Mol. Phys.*, 1997, **92**, 477–488.
27 S. Goedecker, M. Teter and J. Hutter, *Phys. Rev. B: Condens. Matter Mater. Phys.*, 1996, **54**, 1703–1710.
28 M. Krack, *Theor. Chem. Acc.*, 2005, **114**, 145–152.
29 J. VandeVondele and J. Hutter, *J. Chem. Phys.*, 2007, **127**, 114105.
30 J. P. Perdew, K. Burke and M. Ernzerhof, *Phys. Rev. Lett.*, 1996, **77**, 3865–3868.
31 S. Grimme, J. Antony, S. Ehrlich and H. Krieg, *J. Chem. Phys.*, 2010, **132**, 154104.
32 S. Grimme, S. Ehrlich and L. Goerigk, *J. Comput. Chem.*, 2011, **32**, 1456–1465.
33 P. Bultinck, C. Van Alsenoy, P. W. Ayers and R. Carbó-Dorca, *J. Chem. Phys.*, 2007, **126**, 144111.
34 G. J. Martyna and M. E. Tuckerman, *J. Chem. Phys.*, 1999, **110**, 2810–2821.